ARCHIVES OF ACOUSTICS
Vol. **39**, No. 2, pp. 177–187 (2014)

DOI: 10.2478/aoa-2014-0021

Vibrational Properties of Sundatang Soundboard

Ronald Yusri BATAHONG[(1)], Jedol DAYOU[(2)], Semyung WANG[(3)], Jongsuh LEE[(3)]

[(1)] *Teacher Education Institute of Malaysia Keningau Campus*
Locked Beg 11, 89009, Keningau, Sabah, Malaysia

[(2)] *Energy, Vibration and Sound Research Group (e-VIBS), Faculty of Science and Natural Resources*
Universiti Malaysia Sabah, Jalan UMS
88400 Kota Kinabalu, Sabah, Malaysia; e-mail: jed@ums.edu.my

[(3)] *School of Mechatronics and Information Engineering, Gwangju, Institute of Science and Technology*
261 Cheomdan-gwagiro (Oryong-dong), Buk-gu, Gwangju 500-712, Republic of Korea

(*received March 4, 2013; accepted February 11, 2014*)

This paper presents the measurement of vibrational properties of sundatang soundboard. Sundatang is a plucked stringed traditional musical instrument that is popular among the Kadazandusun communities in Sabah, Malaysia. The vibrational properties of the soundboard are measured using CADA-X impact hammering system in a condition where the instrument is without any string. There are two types of sundatang used in this study; one made from acacia and the other from vitex wood. In this measurement, frequency response functions (FRFs) and modal parameters of the top plate and back plate of this instrument are obtained. It is found that in free edge, fundamental frequency of both plates of acacia sundatang is greater than the vitex sundatang in a range of 112 Hz to 230 Hz. However, in clamped edge (attached to its ribs), it was modified to a lower frequency and closer to each other in the range of 55 Hz to 59 Hz. Another finding is the detection of the excitation of similar mode shape at different resonance frequencies. This phenomenon is termed as Different State of Mode (DSM) which is observed may be because the number of testing points is not enough. Findings of this study provide important information to the study of quality development of this instrument.

Keywords: sundatang, frequency response function, impact testing, mode shape.

1. Introduction

Sundatang is one of the traditional musical heritages in Sabah, Malaysia. It is popular especially among the Rungus ethnic in the district of Kudat and Pitas, and generally among the Kadazandusun communities in Sabah. Thus, quite a number of papers have been published on this instrument relating to the culture of the Kadazandusun communities (Alman, 1961; Liew, 1962; Frame, 1975; 1982; Department of Museum and State Archive of Sabah, 1992; Kating, 1996; Pugh-Kitingan, 1992; 2004). However, most of the previous researches focused on the significance of this instrument to the culture of the Kadazandusun communities. Although there are a few researches that have been conducted on local musical instruments such as by Ismail *et al.* (2006) on kompang, Ong and Dayou (2009) and Tee Hao *et al.* (2013) on sompoton, to this point, there is no known research publication related to the acoustics or vibration property of the instrument.

Sundatang falls in the group of plucked string instruments and has the basics shape of a guitar, but has only two strings. This instrument is usually made of acacia wood and vitex wood (also called the *bogil* among the Rungus ethnic), which are widely available in Sabah. Photo of sundatang is shown in Fig. 1 and its anatomy is shown in Fig. 2. The sundatang in Fig. 1 was made by a well-known sundatang maker in the district of Kudat, Sabah.

The sundatang can be divided into four major parts namely the tail, body, neck and head. The body of sundatang consists of the top plate, back plate, ribs and the bridge. The top plate and back plate, which are called the soundboard, are attached to the ribs and an air cavity is formed between them. Similar to other

Fig. 1. Original Sundatang musical instrument.

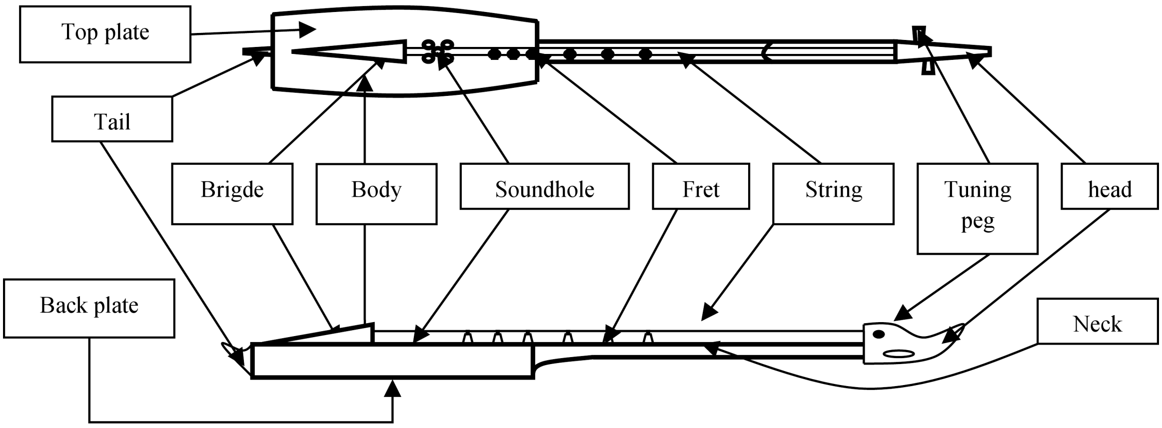

Fig. 2. Anatomy of the original sundatang.

stringed instruments, the function of bridge is to hold the strings of the instrument. There are also four or five small sound holes on the top plate. On the neck of sundatang, there are six fitted frets whose functions are to vary the vibrating length of the string while the instrument is played. The strings of sundatang are stretched between the bridge and the tuning peg on the head that is used to adjust the tension. The tail, top plate, bridge, neck and head of the sundatang are usually made of a single piece of wood, whereas the back plate and tuning peg are made of a different piece. The sundatang is played by plucking its strings with fingers or wooden plectrum. Traditionally, sundatang is used to play a melancholy music (music of expressing sadness) of the Rungus by the sundatang player.

The purpose of this research is to study the vibrational properties of the soundboard (top plate and back plate) of acacia and vitex sundatang, both in a free edge and clamped edge condition without the string attached. Measurements of the vibrational modes of stringed musical instruments such as interference holographic technique and Chaldni powder patterns technique are widely discussed in detail by many researchers (Fletcher, Rossing, 1998; Firth, 1977; Cladersmith, 1978; McIntyre, Woodhouse, 1978; Talbot, Woodhouse, 1997; Jansson, 1969). In this paper, the vibrational properties of sundatang are studied by measuring the modal parameter of the instrument using CADA-X impact hammering system. FRFs of both plates are calculated and displayed, and the vibrational modes of the plates are animated to determine the shapes.

This paper is arranged in 5 sections. Following this introduction there is a brief review on the measurement of modal parameter from a set of FRF measurements in Sec. 2. The experimental method to measure the modal parameter using CADA-X impact hammering system is described in Sec. 3, and the experimental results are discussed in Sec. 4, which highlights several important findings. The paper ends with a brief conclusion in Sec. 5. This study provides an understanding of the significance vibrational properties of the instrument.

2. Modal parameter

Modes or resonances are inherent properties of a structure, which are independent to the forces or loads acting on the structure. Modes are determined by the material properties (mass, stiffness, and damping properties), and also boundary conditions of the structure. Each mode is defined by a natural frequency, modal damping and a mode shape, which is called modal parameters. The modal parameters are obtained from a set of FRF measurement. The FRF describes the input-output relationship between two points on a structure as a function of frequency as discussed in detail by Schwarz, Richardson (1999a; 1999b), Richardson (1997), McHargue, Richardson (1993), Gade, Herlufsen (1992), Ahn *et al.* (2004), Kromulski, Hojan (1996), Bae *et al.* (2011), Devriendt, Guillaume (2007), Pandey *et al.* (1991), Skrodzka *et al.* (2006; 2011; 2013), Lee, Shin (2002), Schoukens *et al.* (2006). The FRF is a measurement of how much displacement, velocity, or acceleration response of a structure at an output point, per unit excitation force at an input point, as illustrated in Fig. 3. This figure also indicates that FRF is defined as the ratio of the Fourier transform of an output response ($X(\omega)$) divided by the Fourier transform of the input force ($F(\omega)$) that caused the output.

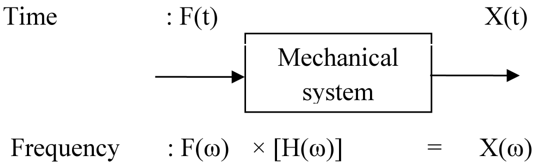

Fig. 3. Block diagram of an FRF (Schwarz, Richardson, 1999b).

The FRF is computed by dividing the cross power spectrum estimate between input and output with the input power spectrum estimate. Mathematically, it is written as

$$\text{FRF} = H(j\omega) = S_{x,f}(j\omega)/S_{f,f}(j\omega) \tag{1}$$

where $S_{x,f}(j\omega)$ – average cross power spectrum between output and input, $S_{f,f}(j\omega)$ – average auto power spectrum of input, and $j\omega$ – frequency variable.

Depending on whether the response motion is measured as displacement, velocity, or acceleration, the FRF and its inverse can have a variety of names such as compliance (displacement/force), mobility (velocity/force), inertance or receptance (acceleration/force), and dynamic stiffness (1/compliance). Each FRF measurement is computed between a sampled input signal and a sampled output signal. To obtain the mode shapes for a structure, a minimum set of FRF measurements must be taken either as a single (fixed) input and many outputs, or between a single (fixed) output and many inputs. The modal parameters of a structure can be obtained by curve fitting a set of FRFs as discussed in detail by Schwarz, Richardson (1999a; 1999b) and Richardson (1997).

3. Experiment setup

In this study, two sundatangs were used which were made of acacia wood and vitex wood. The sundatangs were specially made by the sundatang maker (the maker of the sundatang in Fig. 1) to accommodate the purpose of this experiment. These sundatangs have similar shape and dimensions with the original sundatang as shown in Fig. 1. However, they have a special characteristic, that is their top plate and back plate are detachable from the ribs as shown in Fig. 4. Originally, only the back plate is detachable, whereas the top plate is fixed to the ribs of the sundatang (as shown in Fig. 1 and Fig. 2). The bridge of the sundatang was glued to the top plate and a rectangular space on the top plate where the bridge was located was cut off. At another end of the plate, smaller rectangular shape was cut for the installation of the neck of the sundatang (Fig. 4). The bridge was screwed to the body of the instrument to allow the strings (which were connected from the bridge to the neck) to be undisturbed when the top plate is detached from its ribs. This characteristic enables the measurement of modal parameter of the sundatang top plate and back plate to be carried out in a free edge condition (detached from its ribs) and clamp edge condition (attached to its ribs). Both plates were attached to the sundatang body by screwing them to its ribs. For the acacia sundatang, the top plate mass is 230 g, the back plate mass is 260 g and the total mass of the instrument is 1080 g. Whereas, for the vitex sundatang, the top plate mass is 360 g, the back plate mass is 320 g and the total mass of the instrument is 1550 g. Density of the both type woods was measured, and the result obtained is that density of the acacia wood is 0.51 gcm^{-3} and the vitex wood is 0.72 gcm^{-3}. Other important physical dimensions of the instruments are as shown in Table 1.

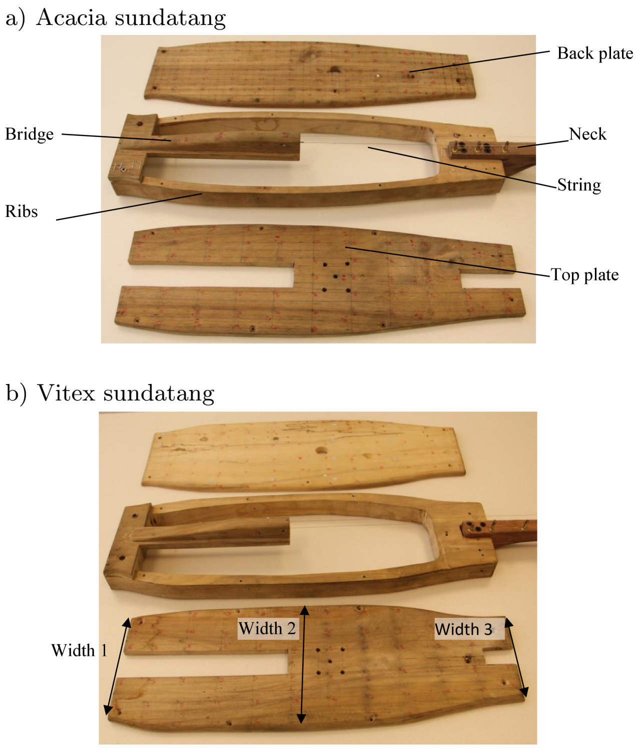

Fig. 4. Photo of the modified sundatang that were used in the experiment.

Table 1. Physical dimensions of sundatang musical instrument used in the experiment.

Physical dimension	Acacia sundatang [cm]	Vitex sundatang [cm]
Total length	106.0	110.1
Length of body	45.8	47.8
Length of neck	41.0	38.8
Width 1	10.0	13.0
Width 2	13.0	15.4
Width 3	8.1	10.2
Length of top plate	42.2	44.0
Length of back plate	45.8	47.8
Thickness of top plate	0.97	0.95
Thickness of back plate	0.94	0.85
Thickness of ribs	1.04	1.36
Height of ribs	2.8	2.8

Modal testing on sundatang using CADA-X impact hammering system was carried out at the Intelligent System Design Laboratory (ISD), Gwangju Institute of Science and Technology, South Korea. Mode shapes of sundatang which are determined by this system were calculated using the Eq. (1). The CADA-X system consists of several major components; they are a hammer, accelerometer, amplifier or signal conditioner, data acquisition system (VXI), and a computer installed with CADA-X software. The arrangement of the system is shown in Fig. 5. The accelerometer that was used in this experiment is B&K charge accelerometer type 4393 with 2.3 g (0.085oz) mass and 0.3159 pC/ms^{-2} or 3.098 pC/g sensitivity. The mass of the accelerometer was less than 10% of the mass of the top plate or the back plate of the both sundatangs. The ratio value enhances the assumption that the accelerometer is acceptable to be used in this measurement without major interruption to the vibrational excitation.

The number of test points on the top plate of acacia sundatang is 59 points, and the back plate is 63 points, the distance between each point is 2 cm (parallel direction to the length of the sundatang) and 4 cm (parallel direction to the width direction of the sundatang). Whereas, for the vitex sundatang, the number of test points on the top plate is 61 points and the back plate is 60 points, the distance between each point is 3 cm (parallel direction to the length of the sundatang) and 4 cm (parallel direction to the width of the sundatang). The test points or hammering points on the top plate and back plate of the sundatang were marked evenly as shown in Fig. 6 as an example for the back plate of acacia sundatang. The geometry that was created in the CADA-X software as shown in Fig. 7 was approximately to the shapes of the back plate (the example in Fig. 6). A few points on the square geometry (1, 2, 3, 5, 10, 11, 67, 68, 70, 76 and 77) were deleted to obtain the shapes of the back plate (Fig. 7). Number of nodes in the CADA-X software were made to equal to the number of hammering points on the plate of the sundatang. One point on each of the top plate and back plate was chosen as a response point, where an accelerometer was mounted on it. This point was chosen by assuming that it is out of nodal point and measurement at this point gives the best repeatable frequencies of peaks in FRFs. For example in Fig. 7, the accelerometer was positioned at point between points 49 and 50 which was fulfilled the assumption. The accelerometer was attached using heavy duty glue to ensure that the accelerometer responses optimally to the vibration of the plate.

a) Experiment arrangement

b) Schematic diagram of CADA-X system

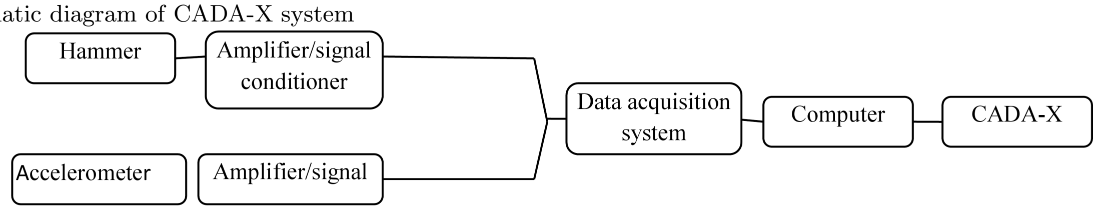

Fig. 5. Modal testing using CADA-X impact hammering experiment set up.

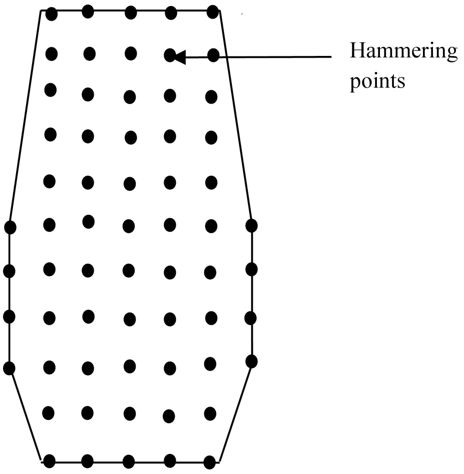

Fig. 6. Hammering points on the back plate of acacia sundatang are marked evenly.

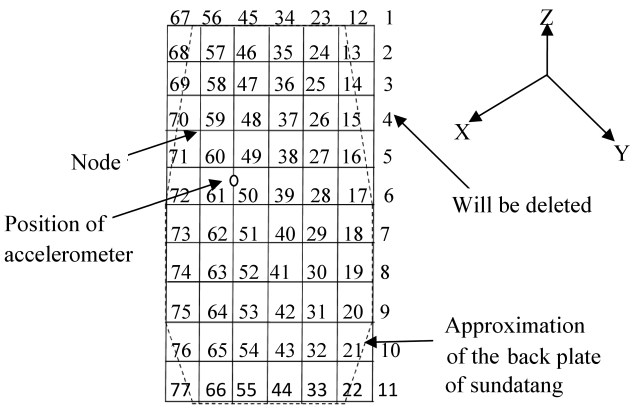

Fig. 7. The corresponding geometry to back plate created in the CADA-X system.

In this experiment, two active channels were used, the 1st channel is for input signals (signal from the hammering points) and the 2nd channel is for the response signals (signal from the response point). Frequency resolution of the FRF measurement is 1 Hz and FFT size is 1024 Hz. Number of averaging of the measurement is a maximum of 5 and frequency interval of the measurements is 0–1024 Hz. The measurements were carried in frequency domain because it is quicker to obtain the convergence of averaging.

Main assumption of this modal analysis is the system is linear. As discussed by Skrodzka *et al.* (2013), in terms of the modal analysis, linearity means that interchanging the positions of the accelerometer and the impact hammer does not change the course of frequency response functions (FRFs) obtained at these two positions. The input signals and the response signals were measured perpendicularly to the plate surfaces. Calculation of frequency response functions (FRF)s were made in the CADA-X software and FRF graphs and animations were produced which are important in determining the modal parameter of the sundatang sounboard.

4. Result and discussion

In order to set out the top plate and back plate in a free edge condition, they were detached from the sundatang body and hung on a high beam with thread as shown on the right most in Fig. 5a. On the other hand, to set out the top plate and the back plate in a clamped edge condition, they were reattached (screwed) to the sundatang body. Then, the sundatang was hung on the high beam again with thread, allowing it vibrate freely as a system when it was knocked with impact hammer tester. In this experiment, FRFs of the top plate and back plate of the acacia and vitex sundatang, set out in a free edge and clamped edge condition are obtained. Figure 8 and Fig. 9 are examples of the obtained FRFs and modal parameter of the top plate of acacia sundatang in free edge, and Fig. 10 and Fig. 11 are examples of the obtained FRFs and modal parameters of the back plate of vitex sundatang in free edge. The FRFs in

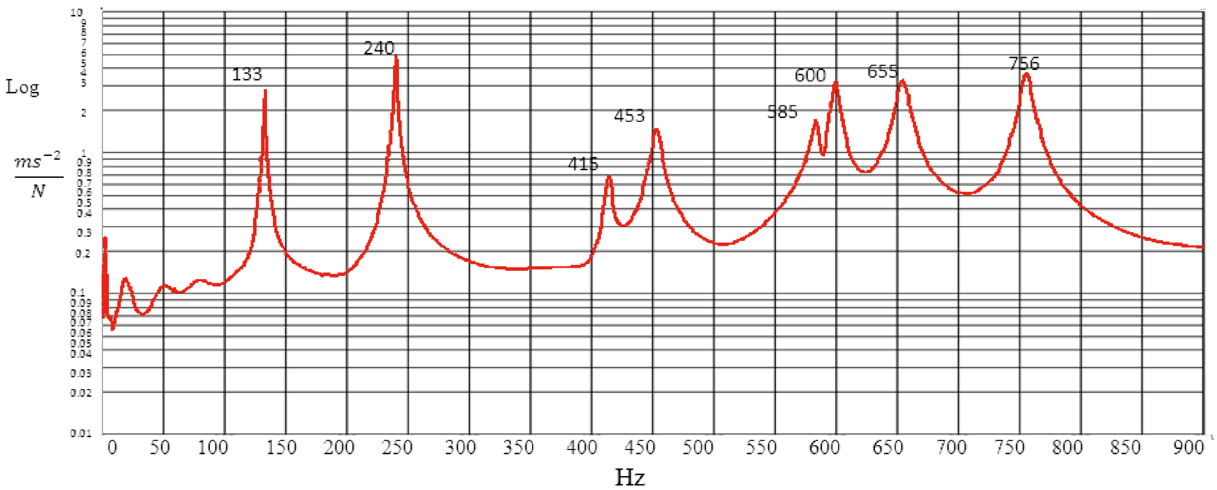

Fig. 8. FRF of top plate (free edge) of acacia sundatang.

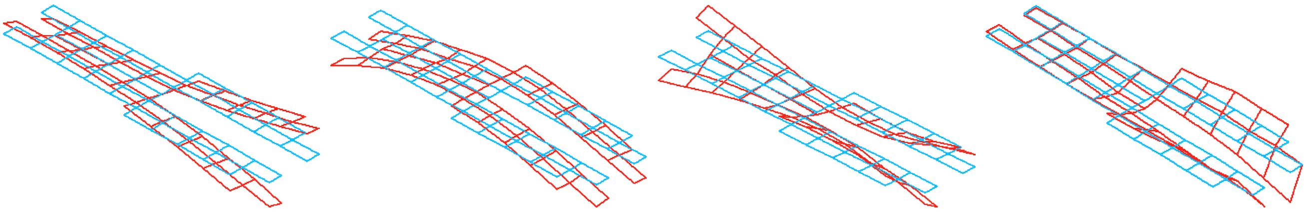

N.F:133 Hz, Damp: 0.65% N.F:240 Hz, Damp: 0.42% N.F:415 Hz, Damp: 0.72% N.F:453 Hz, Damp: 0.90%

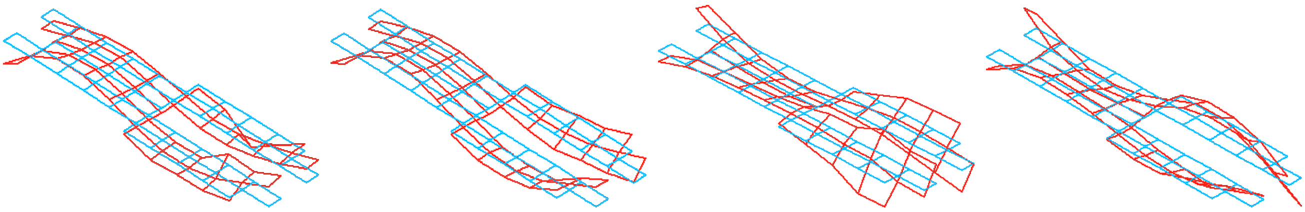

N.F:585 Hz, Damp: 0.60% N.F:600 Hz, Damp: 0.57% N.F:655 Hz, Damp: 0.21% N.F:756 Hz, Damp: 0.61%

Fig. 9. Mode shapes, natural frequencies (N.F) and percentage of critical damping (Damp) of top plate (free edge) of acacia sundatang.

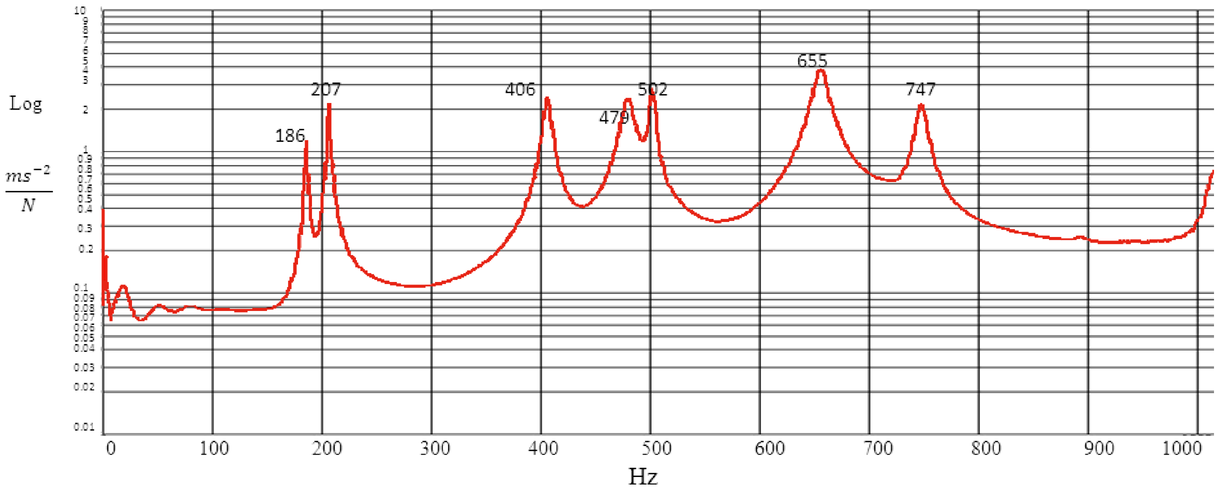

Fig. 10. FRF of back plate (free edge) of vitex sundatang.

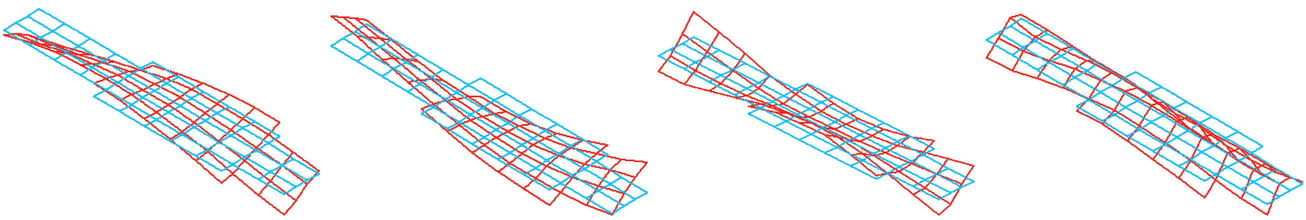

N.F:186 Hz, Damp: 0.62% N.F:207 Hz, Damp: 0.63% N.F:406 Hz, Damp: 0.88% N.F: 479 Hz, Damp: 1.15%

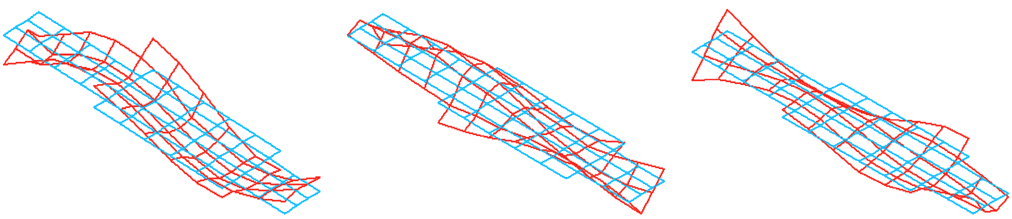

N.F:502 Hz, Damp: 0.46% N.F:655 Hz, Damp: 1.11% N.F:747 Hz, Damp: 0.71%

Fig. 11. Mode shapes, natural frequencies (N.F) and percentage of critical damping (Damp) of back plate (free edge) of vitex sundatang.

Fig. 8 and Fig. 10 were measured from a combination of all testing points on the surface of the top plate and back plate, respectively. The FRFs were calculated between all input signals (at the excitation points) and response signals (at the response point). Mode number of the top plate and back plate of the sundatang were identified approximately to the rectangular plate by (m, n), where m and n are the numbers of nodal lines in the y and x directions, respectively (Fletcher, Rossing, 1998). The mode shapes of the sundatang were determined by scrutinizing the dominant nodal lines on the animated mode shapes of the top plate and back plate. Modal parameters (60 natural frequencies, modal damping, mode shapes) of the top plate and back plate of the acacia and vitex sundatang were identified both for free edge and clamped edge condition as shown in Fig. 12 to Fig. 19. Fifty eight of the modal parameters, except two modal parameters of the back plate of vitex sundatang in clamped edge in Fig. 19 are having the critical modal damping less than 10%. This means, the sundatang system can be treated as a linear system (Skrodzka *et al.*, 2009; Ewins, 1995 in Skrodzka *et al.*, 2013).

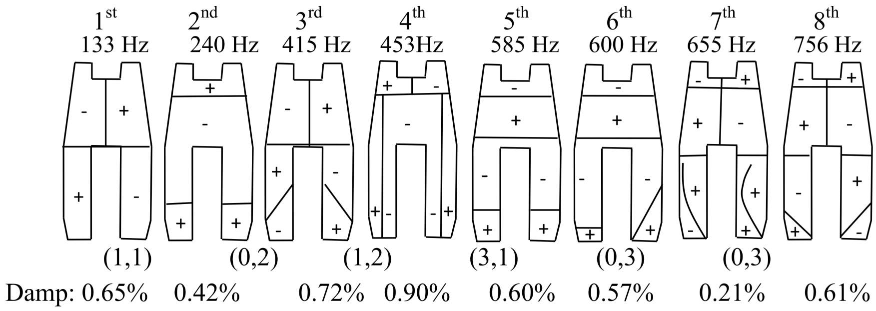

Fig. 12. Mode shapes of the top plate of acacia sundatang in free edge.

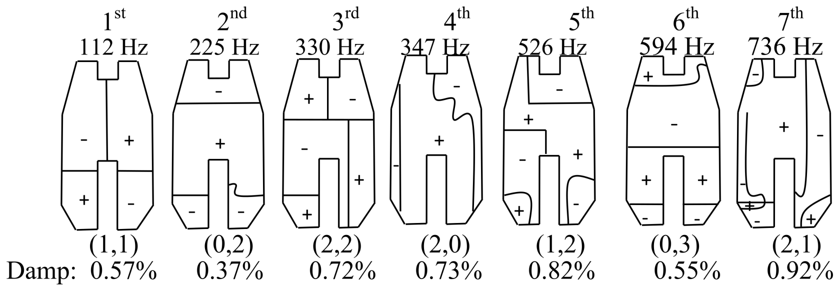

Fig. 13. Mode shapes of the top plate of vitex sundatang in free edge.

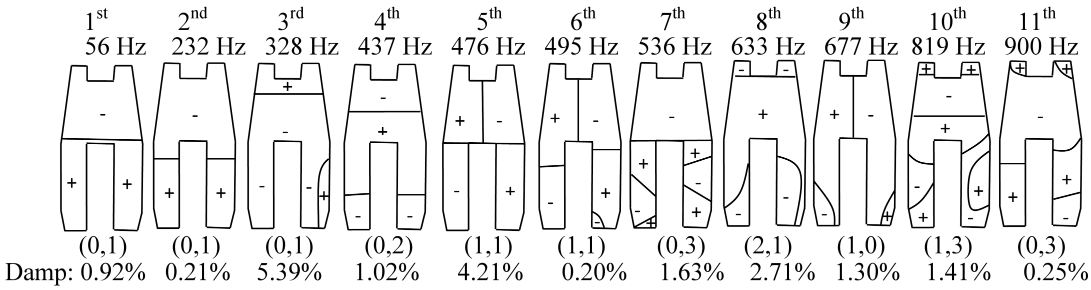

Fig. 14. Mode shapes of the top plate of acacia sundatang in clamped edge.

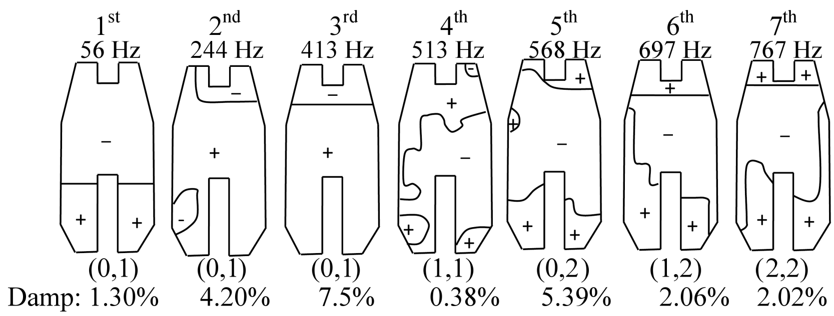

Fig. 15. Mode shapes of top plate of vitex sundatang in clamped edge.

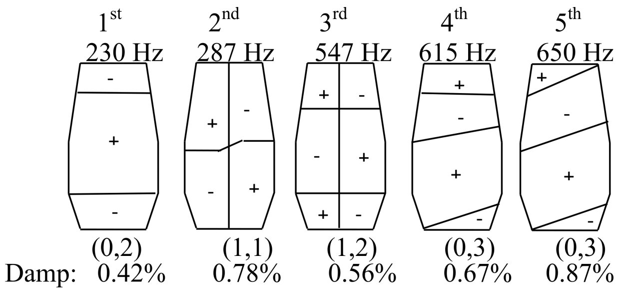

Fig. 16. Mode shapes of back plate of acacia sundatang in free edge.

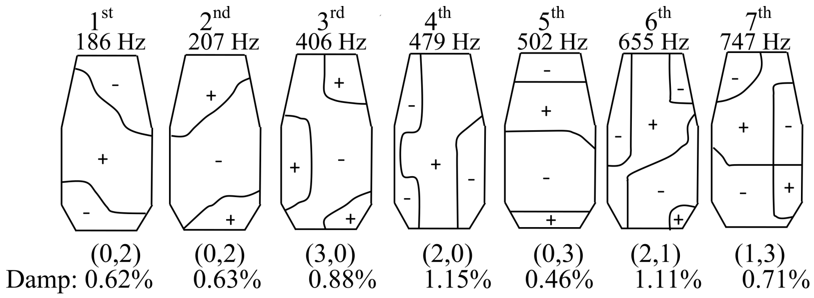

Fig. 17. Mode shapes of back plate of vitex sundatang in free edge.

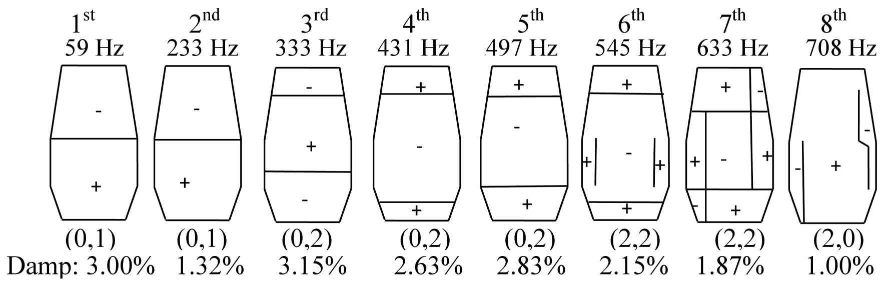

Fig. 18. Mode shapes of back plate of acacia sundatang in clamped edge.

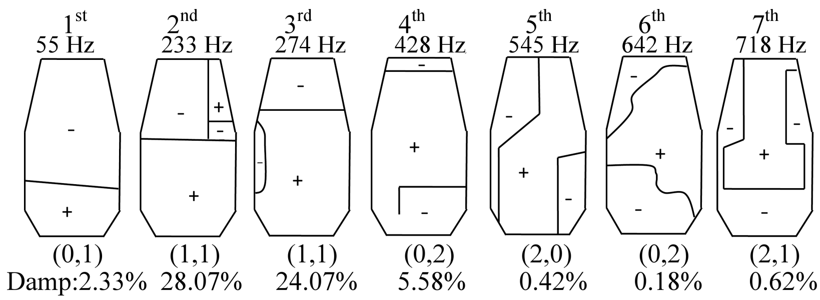

Fig. 19. Mode shapes of back plate of vitex sundatang in clamped edge.

From these figures, it is found that, the number of modes of the top plate and the back plate in free edge condition of the acacia sundatang in frequency range of 0 Hz to 1000 Hz has changed, when they were attached to the body of the sundatang (clamped edge). It is noted that the number of modes of the top plate in the free edge condition is eight (Fig. 12) whereas in the clamped edge is eleven (Fig. 14). Similarly, the number of modes of the back plate in a free edge condition is five (Fig. 16) whereas in clamped edge is eight (Fig. 18). On the contrary, the number of modes of the top plate and back plate of the vitex sundatang is equal before (free edge) and after (clamped edge) being attached to the ribs of the sundatang as shown in Fig. 13, Fig. 15, Fig. 17 and Fig. 19.

It is also found that the fundamental frequency of top plate and back plate of the acacia sundatang is greater than the vitex sundatang in free edge as shown in the third row of Table 2. The fundamental frequencies of the top plate and the back plate of the both sundatangs are in the frequency range of 112 Hz to 230 Hz. However, when both plates were attached to the ribs (in clamped edge), their fundamental frequency were modified and became lower and closer to each other in the range of 55–59 Hz as shown in the fourth row of Table 2 and Fig. 12 to Fig. 19. Besides

Table 2. Fundamental resonance frequency of the both plates of sundatang.

Condition	Acacia Sundatang		Vitex sundatang	
	Top plate [Hz]	Back plate [Hz]	Top plate [Hz]	Back plate [Hz]
Free edge	133	230	112	186
Clamped edge	56	59	56	55

that, the number of their mode shape also changed from higher number to (0,1). For example, the mode shape of the fundamental frequency of the top plate of the acacia (1st mode = 133 Hz in Fig. 12) and vitex sundatang (1st mode = 112 Hz in Fig. 13) in free edge is (1,1), thus was modified to (0,1) when they were attached to the ribs of this instrument as shown in Fig. 14 (1st mode = 56 Hz for acacia) and Fig. 15 (1st mode = 56 Hz for vitex). Similarly, the mode shape of the fundamental frequency of the back plate of the acacia (1st mode = 230 Hz in Fig. 16) and vitex sundatang (1st mode = 186 Hz in Fig. 17) in free edge is (0,2), was modified to (0,1) when they were attached to the ribs as shown in Fig. 18 (1st mode 59 Hz for acacia) and Fig. 19 (1st mode = 55 Hz for vitex). The above findings bring us to the conclusion that the number of mode, frequency modes, mode shape number and their sequence are changed after changing the boundary condition of sundatang soundboards which is from free edge to clamped edge condition.

Another finding in this paper which is the detection of similar mode shapes at different resonance frequencies. This finding is similar to the finding reported by Ando (1986), cited by Fletcher and Rossing (1998), and by Ramakrisna and Sondhi (1954). In this paper, this phenomenon is termed Different State of Mode or DSM. In order to describe the phenomenon, the resonance frequency with perfect mode shapes is called the Fundamental State of Mode (FSM) and the resonance frequency after, having similar mode shape to the FSM is called Higher State of Mode (HSM). The FSM and HSM in general have similar mode pattern but different in actual shape.

Figure 18 shows the best example on the occurrences of this phenomenon. From this figure, the 3rd mode of the back plate of the acacia sundatang set in clamped edge with perfect mode shape of (0,2) is the FSM. On the other hand, the 4th mode with an imperfect mode shape of (0,2), which is different in actual shape, is the 1st HSM, whereas the 5th mode (also with an imperfect shape of (0,2) also different from the actual shape) is the 2nd HSM. Further inspections of the modal parameters in Fig. 12 to Fig. 19 show that, for the acacia sundatang, its top plate has one mode with DSM in free edge which is the (0,3) and three modes with DSM in clamped edge which are the (0,1), the (1,1) and the (0,3). The (0,1) mode (in clamped edge of top plate) has three DSMs that consists of FSM at 55.92 Hz and two HSMs at 232.21 Hz (1st HSM) and at 328.11 Hz (2nd HSM). Similar observation can be implied to the vitex sundatang plate. The occurrences of this phenomenon are summarized in Table 3 and Table 4 for acacia and vitex sundatang, respectively. The num-

Table 3. Different State of Modes (DSMs) of the top and back plates of acacia sundatang that consists of Fundamental State of Mode (FSM) and Higher State of Mode (HSM).

Condition	Top plate			Back plate		
	FSM	1st HSM	2nd HSM	FSM	1st HSM	2nd HSM
Free edge	5th (0,3) 585 Hz	6th (0,3) 600 Hz	–	4th (0,3) 615 Hz	5th (0,3) 650 Hz	–
Clamped edge	1st (0,1) 56 Hz	2nd (0,1) 232 Hz	3rd (0,1) 328 Hz	1st (0,1) 59 Hz	2nd (0,1) 233 Hz	–
	5th (1,1) 476 Hz	6th (1,1) 495 Hz	–	3rd (0,2) 333 Hz	4th (0,2) 431 Hz	5th (0,2) 497 Hz
	7th (0,3) 536 Hz	11th (0,3) 900 Hz	–	6th (2,2) 545 Hz	7th (2,2) 633 Hz	–

Table 4. The occurrences of DSMs for vitex sundatang.

Condition	Top plate			Back plate	
	FSM	1st HSM	2nd HSM	FSM	1st HSM
Free edge	–	–	–	1st (0,2) 186 Hz	2nd (0,2) 207 Hz
Clamped edge	1st (0,1) 56 Hz	2nd (0,1) 244 Hz	3rd (0,1) 413 Hz	2nd (1,1) 233 Hz	3rd (1,1) 274 Hz
	–	–	–	4th (0,2) 428 Hz	6th (0,2) 642 Hz

ber of detected DSMs increased when the sundatang plate is attached to its body. For example, from Table 3, there are a maximum of two DSMs for both top and back plates of acacia sundatang. However, when the plates are attached to the ribs, which is in clamped edge condition, three maximum DSMs can be found from each plate. Similar finding can be seen from Table 4 for vitex sundatang. The DSMs was observed may be because the number of testing points is not enough.

5. Conclusion

The vibrational properties of soundboard (top and back plates) of acacia and vitex sundatang without any strings were investigated. This study was carried out to find the vibrational properties of the both plates of the acacia and vitex sundatang in a free edge and clamped edge condition. The vibrational properties of the soundboard were measured using CADA-X impact hammering system. The obtained FRFs and mode shape animations of the top plate and back plate were securitized to determine their modal parameters (natural frequency, mode shape and modal damping). Hence, we can conclude that:

1. For the top plate and back plate of the acacia sundatang, their number of modes in the frequency range of 0 Hz to 1000 Hz is changed when they were clamped to its ribs. However, in this study, this pattern did not happen to the vitex sundatang.
2. Fundamental natural frequency of the top plate and back plate of the acacia sundatang is greater than the vitex sundatang in free edge and in the range of 112 Hz to 230 Hz. However, their fundamental natural frequency was modified and became lower and closer to each other in the range of 55 Hz to 59 Hz in a clamped edge (attached to its ribs).
3. Phenomenon of similar mode shapes at different resonance frequency which is termed as Different State of Modes (DSMs) was detected in this study. This phenomenon may be due to mode overlap, which is observed because the number of testing points is not enough. Further study of the DSMs could be carried out by measurement with addition more of the testing points or using visualizations at higher resolution than the CADA-X system.

Findings of this study are very significant knowledge of the vibrational properties of sundatang soundboard, which can be used in the advancement studies towards a better quality of sundatang musical instrument.

References

1. Ahn S.J., Weui B.J., Wan S.Y. (2004), *Unbiased expression of FRF with exponential Window Function in Impact Hammer Testing*, Journal of Sound and Vibration, **277**, 931–941.
2. Alman J.H. (1961), *If you can't sing, you can beat a gong*, Sabah Society Journal, **2**, 29–42.
3. Bae W., Kyong Y., Dayou J., Park K., Wang S. (2011), *Scaling the Operating Deflection Shapes Obtained from Scanning Laser Doppler Vibrometer*, Journal of Nondestructive Evaluation, **30**, 2, 91–98.
4. Cladersmith G. (1978), *Guitar as a reflex enclosure*, Journal of Acoustical Society of America, **63**, 5, 1566–1575.
5. Department of Museum and State Archive of Sabah (1992), *An introduction to the traditional musical instruments of Sabah*, pp. 1–23, Kota Kinabalu.
6. Devriendt C., Guillaume P. (2007), *The use of transmissibility measurements in output-only modal analysis*, Mechanical System and Signal Processing, **21**, 2689–2696.
7. Firth I.M. (1977), *Physics of the guitar at the Helmholtz and first top-plate resonances*, Journal of Acoustical Society of America, **61**, 2, 588–593.
8. Fletcher N.H., Rossing T.D. (1998), *The physics of musical instruments*, 2nd edition. Springer-Verlag, New York, pp. 239–326.
9. Frame E.M. (1975), *A preliminary survey of several major musical instruments and form-types of Sabah, Malaysia*, Borneo Research Bulletin, **7**, 1, 16–24.
10. Frame E.M. (1976), *Several major musical instruments of Sabah, Malaysia*, Journal of the Malaysian, Branch of the Royal Asiatic Society, Volume XLIX, Part 2.
11. Frame E.M. (1982), *The musical instruments of Sabah, Malaysia*, Society of Ethnomusicology, Inc., 247–274.
12. Gade S., Herlufsen H. (1992), *Errors involved in computing impulse response functions via frequency response function*, Mechanical systems and Signal Processing, **6**, 3, 193–206.
13. Ismail A., Samad S.A., Hussain A., Azhari C.H., Zainal M.R.M. (2006), *Analysis of the Sound of the Kompang for Computer Music Synthesis*, 4th Student Conference on Research and Development (SCOReD 2006), IEEE, pp. 95–98, Malaysia.
14. Jansson E.V. (1969), *A comparison of acoustical measurements and hologram interferometry measurements of the vibrations of a guitar top plate*, Journal STL-QPSR, **10**, 2–3, 36–41.
15. Kating P.K. (1996), *Traditional musical instrument in Sabah our cultural heritage*, [in Malay], KDI Publications Sdn. Bhd, pp. 90–94, Kota Kinabalu.
16. Kromulski J., Hojan E. (1996), *An application of two experimental modal analysis methods for the determination of operational deflection shapes*, Journal of Sound and Vibration, **196**, 4, 429–438.
17. Lee U., Shin J. (2002), *A frequency response function-based structural damage identification method*, Computers and Structures, **80**, 117–132.

18. Liew R. (1962), *Music and musical instruments in Borneo*, Borneo Society Journal, **5**, 10–17.

19. McHargue P.L., Richardson M.H. (1993), *Operating deflection shapes from time versus frequency domain measurement*, 11th IMAC Conference, pp. 108, Kissimmee, FL.

20. McIntyre M.E., Woodhouse J. (1978), *The acoustics of stringed musical instruments*, Interdisciplinary Science Reviews, **3**, 2, 157–173.

21. Ong C.W., Dayou J. (2009), *Frequency Characteristic of Sound from Sompoton Musical Instrument*, Borneo Science, **25**, 71–79.

22. Pandey A.K., Biswas M., Samman M.M. (1991), *Damage detection from changes in curvature mode shapes*, Journal of Sound and Vibration, **145**, 2, 321–332.

23. Pugh-Kitingan J. (1992), *Musical instruments in the cultural heritage of Sabah*, Borneo Research Council Second Biennial International Conference, pp. 1–13, Kota Kinabalu.

24. Pugh-Kitingan J. (2004), *Selected papers on music in Sabah.* Universiti Malaysia Sabah, Kota Kinabalu, pp. 19–42.

25. Ramakrisna B.S., Sondhi M.M. (1954), *Vibrations of Indian musical drums regarded as composite membranes*, Journal of the Acoustical Society of America, **26**, 4, 523–528.

26. Richardson M.H. (1997), *Is it a shape, or an operating deflections shape?*, Sound and Vibration Magazine 30th Anniversary Issue, Vibrant Technology, Inc., Jamestwon, California, pp. 1–11.

27. Schoukens J., Rolain Y., Pintelon R. (2006), *Analysis of window leakage effects in frequency response function measurements*, Automatica, **42**, 27–38.

28. Schwarz B.J., Richardson M.H. (1999a), *Introduction to operating deflection shapes*, CSI Reliability Week, Orlando, FL, pp. 1–7.

29. Schwarz B.J., Richardson M.H. (1999b), *Experimental modal analysis*, CSI Reliability Week, Orlando, FL, pp. 1–12.

30. Skrodzka E.B., Hojan E., Proksza R. (2006), *Vibroacustics investigation of a batter head of a snare drum*, Archives of Acoustics, **31**, 3, 289–297.

31. Skrodzka E.B., Linde B.B.J., Krupa A. (2013), *Modal parameters of two violins with different varnish layers and subjective evaluation of their sound quality*, Archives of Acoustics, **38**, 1, 75–81.

32. Skrodzka E., Lapa A., Linde B.B.J., Rosenfeld E. (2011), *Modal parameters of two incomplete and complete guitars differing in the bracing pattern of the soundboard*, Journal of Acoustical Society of America, **130**, 4, 2186–2195.

33. Talbot J.P., Woodhouse J. (1997), *The Vibration damping of laminated plates*, Elsevier, composites part A, 28, A, 1007–1012.

34. Wong T.H., Dayou J., Ngu M.C.D., Chang J.H.W., Liew W.Y.H. (2013), *Clamped bar model for sompoton vibrator*, Archives of Acoustics, **38**, 3, 425–432.